Magnetic properties of Mn δ-doped GaAs

[1]Hirak Kumar Chandra, [2]Shahnewaz Mondal, [1]Basir Ahamed Khan

[1, 3]Department of Physics, Krishnath College, Berhampore, Murshidabad, WB, India-742101

[2]Department of Physics, Sripat Singh College, Jiaganj, Murshidabad, WB, India-742123

Email: basir.khan@gmail.com

Abstract : Dilute magnetic semiconductors play crucial roles in next generation magnetic memory devices. GaAs is a well-known wide band gap semiconductor, while doped with Mn, a *d*-block element, in dilute limit, it becomes a dilute magnetic semiconductor. In this context, we have calculated the inter-atomic exchange parameters for Mn δ-doped GaAs heterostructures as a function of layer thickness. The inter-atomic exchange parameters J_1 and J_3 have been come out to be larger in dilute doping cases compared to the larger Mn coverage cases. For 50% δ- doping case the exchange parameter J_1has been found to be 60$\pm$10 meV. This increases to 90$\pm$10 meV at 12.5% doping. The induced magnetic moment on As has been found to die down as one goes beyond four monolayers from the Mn δ-doping layer.

KEYWORDS: Dilute magnetic semiconductor, Mn doped GaAs, Heterostructure, Magnetic properties.

I. INTRODUCTION

Dilute magnetic semiconductors (DMSs) have attracted a lot of research attention in recent times because of the possibility of their applications in many electronic devices [1, 2]. The DMS systems work on the principle of the electronic spin degree of freedom and the new generation electronic devices envisaged go by the name of spintronics devices. The spin degree of freedom of an electron can be utilized in semiconductor technology to develop new-semiconductor materials based on spin-dependent phenomena [3, 4]. Mn doped GaAs is one such DMS system which has been studied with the aim of fabricating spintronic devices. However, the use the Mn doped GaAs systems were limited because of their very low ferromagnetic ordering temperature (T_C) [5]. A lot of experimental effort has been directed in making DMS materials which can exhibit room temperature ferromagnetism. It has been reported that the ferromagnetic Curie temperature and the spontaneous magnetization of DMS materials depends on the distribution of magnetic impurities and some external biased potential [6]. Based on this idea, *TC* can be enhanced significantly in some low dimensional DMS systems. A possible way to achieve this is to synthesize DMS materials in which, a two dimensional layer with doped magnetic atoms has been sandwiched between bulk heterostructure materials. A δ -doped magnetic heterostructure is nothing but highly doped thin magnetic semiconductor layers followed by thick nonmagnetic semiconductor layers. This type of heterostructures have been found to be of interest because a large number of magnetic ions are concentrated within a thin layer which cannot be realized in a bulk Mn doped GaAs system where one has phase separation. In search for high *TC* DMS materials, Nazmul el al. [7] showed that the magnetic semiconductor heterostructures consisting of Mn δ -doped GaAs and p-type AlGaAs layers exhibit a $T_C$of up to 250 K. Chen et al. [8] fabricated GaSb/Mn digital heterostructures which has been reported to exhibit *TC* higher than the room temperature. There exist reports based on theoretical calculations within mean field approximation, which have predicted that the value of $T_C$can be enhanced with the increase of magnetic dopant concentrations as well as carriers in the semiconductors. It has also been observed from the experiments done by Kawakami et al. [12] that, distribution of Mn within a layer of (Ga,Mn)As heterostructure plays a significant role on determining the $T_C$of the material. But some experiments have shown that during the growth and processing of Mn doped GaAs sample, some intrinsic defects such as As, antisites, As interstitials, Mn interstitials etc., have been produced [9–11]. These defects act as donors which compensate the Mn acceptors in (Ga,Mn)As complex and these suppress the ferromagnetic interactions. To overcome this shortfall, digital ferromagnetic heterostructures have been developed which have much higher Mn concentration than that of bulk Mn doped compounds [12]. Zhou et al. [13] studied the role of an additional confining potential on ferromagnetism in III-V digital ferromagnetic heterostructures by plane wave pseudo potential calculations. They have shown that, the localized hole concentration in the magnetic layer which increases with the additional potential, is responsible for the enhancement of ferromagnetic interactions and higher *TC* of the system. From the experimental studies it has been observed that ferromagnetic properties depend on the thickness and the composition of nonmagnetic layer and in the case of (Ga,Mn)As/GaAs heterostructure, the $T_C$decreases with the increasing GaAs interlayer thickness [14]. In this work, we have theoretically investigated with the help of first principle density functional calculations, what type of magnetic interactions are more favorable when Mn is doped in a layer of (Ga,Mn)As/GaAs heterostructure with various doping concentrations. We also have extracted the interatomic exchange parameters by using the Heisenberg spin model to find how the magnetic interaction strengths vary as a function of layer thickness.

II. METHODOLOGIES

For the calculations, various sizes of GaAs supercell with zinc blende structure have been constructed in which Mn atoms replace the Ga atoms in a particular layer. Different doping concentrations such as, 50%, 25% and 12.5% of Mn in a single layer of GaAs supercell have been taken in this case. The lattice parameter of the unit cell is taken to be the experimental value 5.65 Å [15] and kept fixed during the calculations. The electronic structure calculations have been performed within a plane wave pseudopotential implementation of density functional theory as implemented in VASP [16–18] within PAW potentials. GGA PW91 [19] approximation for the exchange correlation has been used as it provides better estimates for the magnetic energy. Various doping concentrations of Mn atoms as stated above, have been taken with different arrangements in a single monolayer of GaAs supercell. Each structure has been relaxed until the Hellmann-Feynman force on individual atom becomes less than 10 meV/Å.

The total energy of each structure with ferromagnetic and different types of antiferromagnetic arrangements has been calculated. These have been mapped to a Heisenberg model to evaluate the interatomic exchange parameters.

The Heisenberg spin model Hamiltonian is written as

$$H = -12\sum_{ij} J_{ij}\vec{s}_i.\vec{s}_j \quad (1)$$

where, $\vec{s}_i$and $\vec{s}_j$denote the spin moment of i-th and j-th atom and J_{ij}denotes the interatomic exchange parameter. If $J$is positive, then the model describes ferromagnetic order, because the spins will tend to be oriented in the same direction to give a positive value of $\langle \vec{s}_i.\vec{s}_j \rangle$and this minimizes the energy. In the opposite case, a negative value of J will lead to antiferromagnetic order. In our calculations the magnitudes of $\vec{s}_i$and $\vec{s}_i$have been absorbed in J.

Here we discuss how to evaluate the exchange parameters for different magnetic configurations –

1. First of all, we have taken 50% substitution of Ga byMn in a single monolayer of GaAs heterostructure grown along z-direction. The Mn arrangements in a single layer are shown in the following picture (Fig.1). Here we have considered a model where the total ground state energy is divided into two components as following

$$E_{FM} = E_0 + E_{spin} \quad (2)$$

where, $E_0$is assumed to be the energy of the nonmagnetic configuration and $E_{spin}$is the spin polarizedenergy.

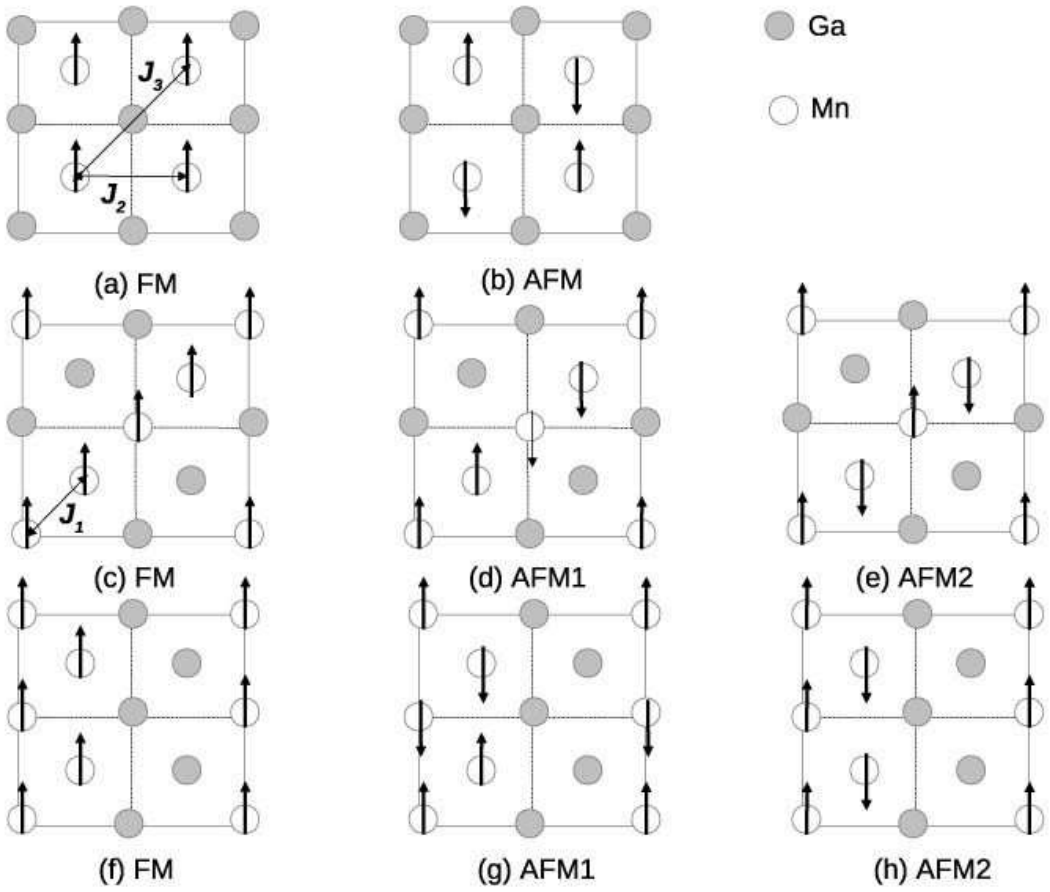

Figure 1:Various types of Mn arrangements in a two dimensional layer of (Ga,Mn)As with 50% coverage have been shown. The grey circles represent the Ga atom and white circles represent the Mn atom in the twodimensional surface. The different spin arrangements of each structure have been shown where ↑ represents theup spin and ↓ represents the down spin moment of the individual atom.

(i) Considering the ferromagnetic spin arrangement as shown in Fig.1(a) the total energy of the supercell can be written as following,

$$E^1_{FM} = E_0 - (8J_2 + 8J_3\ ) \quad (3)$$

where, J_2 and J_3 are 2nd and 3rd nearest neighbor exchange interaction parameters between the Mn atoms. (ii) Similarly, considering the antiferromagnetic spin arrangement of Mn atoms in the same structure as shown in Fig.1(b), the total energy can be written as,

$$E^1_{AFM} = E_0 + (8J_2 - 8J_3\ ) \quad (4)$$

From the above two equations, one can extract the interatomic exchange parameters evaluating the ferromagnetic and antiferromagnetic total energies from ab-initio calculations.

2. Now consider the arrangement of Mn atoms as shown in the Fig.1(c), (d) and (e) for different spin arrangements. From the ferromagnetic and antiferromagnetic spin arrangements we can construct the following set of equations:

$$E^2_{FM} = E_0 + (8J_2 - 8J_3\ ) \quad (5)$$

$$E^2_{AFM1} = E_0 + 8J_3 \quad (6)$$

$$E^2_{AFM2} = E_0 + 4J_2 - 8J_3 \quad (7)$$

From the above equations we can evaluate J_1, J_2 and J_3 for the above Mn arrangement of Mn δ doped GaAs heterostructure.

3. Considering the 3rd type of Mn arrangement in a monolayer of GaAs heterostructure namely chalcopyrite structure as shown in Fig.1 (f), (g) and (h), we can construct the following set of equations:

$$E_{FM}^{3} = E_0 - 4J_1 - 8J_2 \quad (8)$$
$$E_{AFM1}^{3} = E_0 + 4J_2 \quad (9)$$
$$E_{AFM2}^{3} = E_0 + 4J_1 - 4J_2 \quad (10)$$

4. Again considering another type of Mn arrangements as shown in Fig.2(a), (b) and (c),

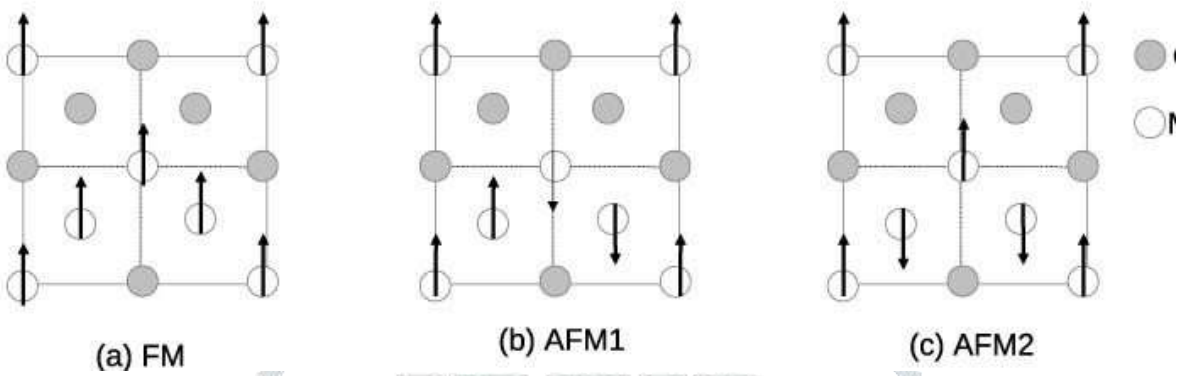

Figure 2: Various types of Mn arrangements in a two dimensional layer of (Ga,Mn)As with 50% coveragehave been shown. The grey circles represent the Ga atoms and white circles represent the Mn atoms in the twodimensional surface. The different spin arrangements of each structure have been shown, where ↑ represents theup spin and ↓ represents the down spin moment of the individual atom.

we can construct the following set of equations for different spin arrangements as,

$$E_{FM}^{4} = E_0 - 4J_1 - 2J_2 - 4J_3 \quad (11)$$
$$E_{AFM1}^{4} = E_0 - 2J_2 + 4J_3 \quad (12)$$
$$E_{AFM2}^{4} = E_0 + 4J_1 - 2J_2 - 4J_3 \quad (13)$$

The interatomic exchange parameters *J*1, *J*2 and *J*3 have been extracted for each arrangement of Mn atoms in a single monolayer of GaAs heterostructure using the above set of equations.

Next, we have considered the case of 25% Mn doping on a single monolayer of GaAs supercell, i.e. 25% Ga atoms in the monolayer are replaced by Mn atoms. We have considered three types of Mn arrangements here.

5. The first type of arrangement of Mn atoms on a monolayer for FM and AFM configurations, which we have considered, are shown in the Fig.3(a) and (b).

Regarding this figure we can construct the following set of equation using the Heisenberg's model Hamiltonian,

$$E_{FM}^{5} = E_0 - J_1 - 2J_3 \quad (14)$$
$$E_{FM}^{5} = E_0 + J_1 - 2J_3 \quad (15)$$

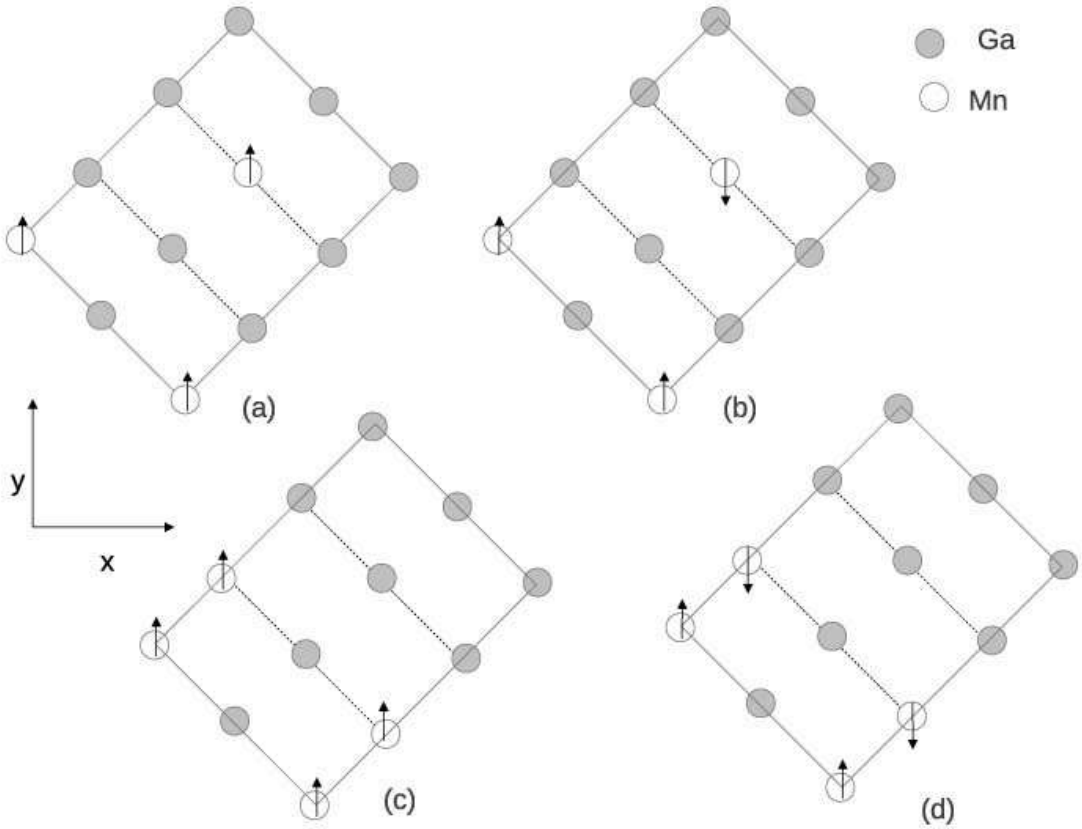

Figure 3: Various types of Mn arrangements in a two dimensional layer of (Ga,Mn)As with 25% coveragehave been shown. The grey circles represent the Ga atoms and white circles represent the Mn atoms in the twodimensional surface. The different spin arrangements of each structure have been shown where ↑ represents theup spin and ↓ represents the down spin moment of the individual atom. The x and y axes have been shown in thefigure to specify the orientation in a two dimensional layer.

6. Considering the second type of Mn arrangements as shown in the Fig.3(c) and (d), we can construct the following equations,

$$E_{FM}^{6} = E_0 - 2J_2 - 2J_3 \quad (16)$$

$$E_{AFM}^{6} = E_0 + 2J_2 - 2J_3 \quad (17)$$

(7) The third type of arrangements which we have considered here is shown in the Fig.4(a) and (b), we can construct the following set of equations,

$$E_{FM}^{7} = E_0 - 4J_3 \quad (18)$$

$$E_{FM}^{7} = E_0 \quad (19)$$

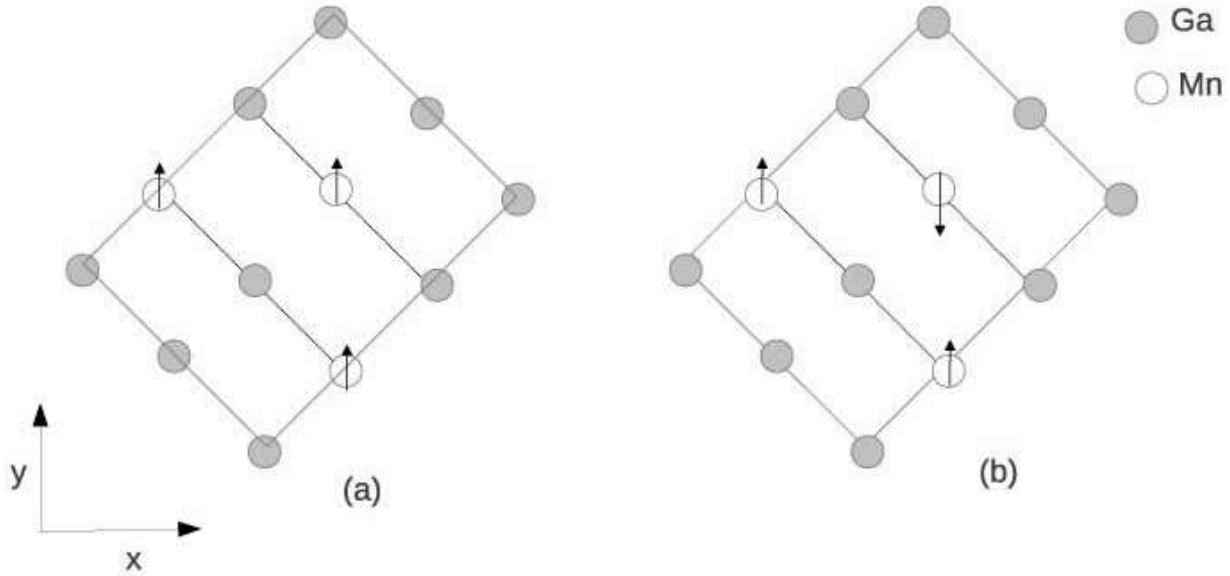

Figure 4: Various types' ofMn arrangements in a two dimensional layer of GaAs with 25% coverage have beenshown. The grey circles represent the Ga atom and white circles represent the Mn atom in the two dimensionalsurface. The different spin arrangements of each structure have been shown where ↑ represents the up spin and ↓ represents the down spin moment of the individual atom.

From these set of equations we can evaluate the interatomic exchange parameters by using the total energies calculated from the first principle calculations.

8. We also have considered the case of 12.5% coverage of Mn atoms in a monolayer of GaAs suupercell. The Mn arrangements are shown in the Fig.5 (a), (b), (c) and (d). From these arrangements as shown in Fig.55 (a) and (b) we can construct the following equations:

$$E_{FM}^{8} = E_0 - 2J_1 \quad (20)$$

$$E_{AFM}^{8} = E_0 + 2J_1 \quad (21)$$

Similarly, considering the arrangements as shown in Fig.5(c) and (d) we can construct the following couple of equations:

$$E_{FM}^{9} = E_0 - J_2 \quad (22)$$

$$E_{AFM}^{9} = E_0 + J_2 \quad (23)$$

With the help of these pair of equations we can find out the value of exchange parameters J_1 and J_2.

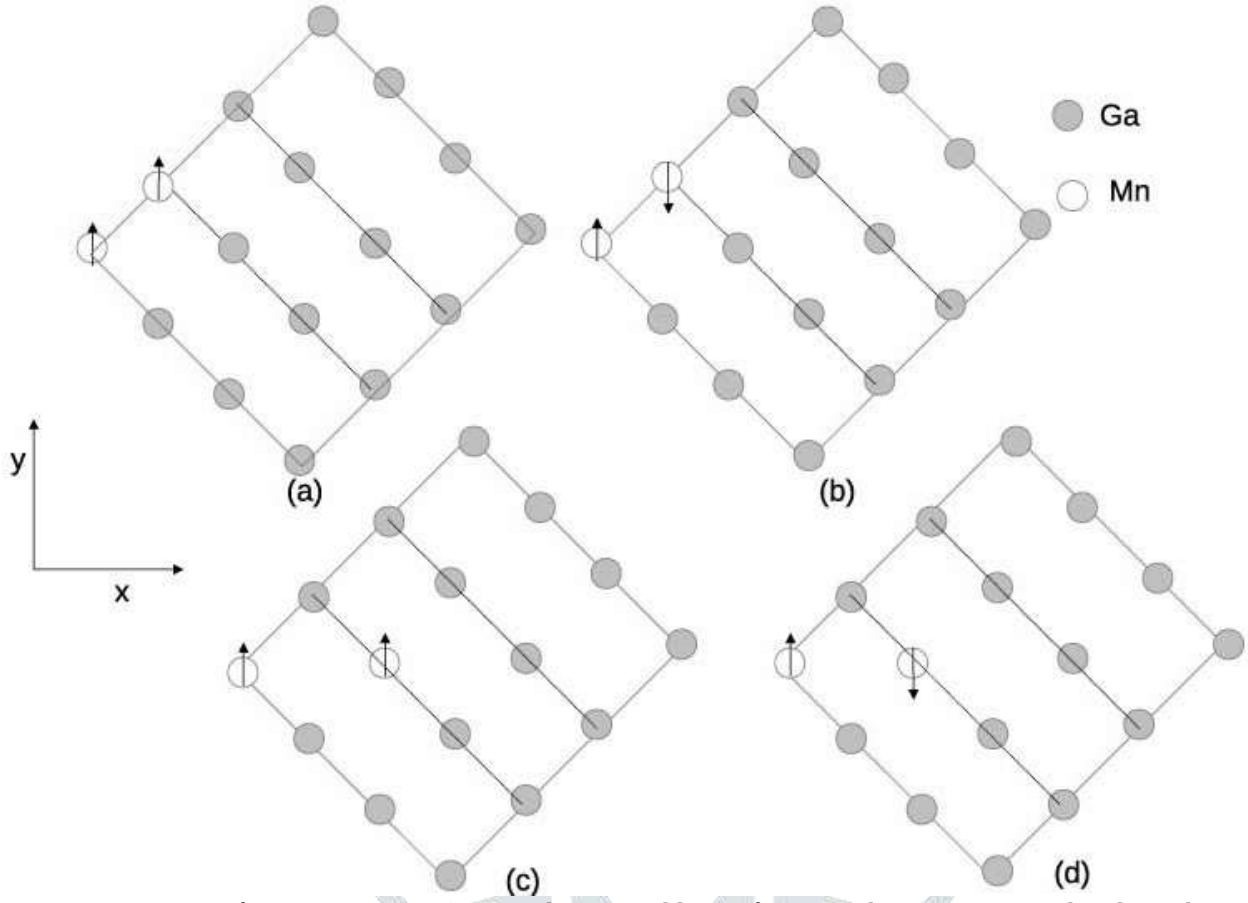

Figure 5: Various types of Mn arrangements in a two dimensional layer of GaAs with 12.5% coverage havebeen shown. The grey circles represent the Ga atom and white circles represent the Mn atom in the two dimensionalsurface. The different spin arrangements of each structure have been shown where ↑ represents the up spinand ↓ represents the down spin moment of the individual atom.

III. RESULTS AND DISCUSSIONS

The total energy for each of the configurations, as shown above, has been calculated from the *ab-initio* density functional theory calculations. These energy data are used to evaluate the values of interatomic exchange parameters J_1, J_2 and J_3 for different configurations.

1. Considering the 1st case (Fig.1 (a), (b)), the total ground state energies of FM and AFM configurations from the *ab-initio* calculations have been calculated for different number of layers grown along z-direction. From these energies, the interatomic exchange parameters (J_2) have been calculated using Eq.3 and Eq.4, and are tabulated in Table.1. From the table it can be seen that the FM configuration are energetically more stable than the AFM configurations. The sign of J_2 (⟨100⟩ direction as shown in Fig.1) from our calculations are matching with the J_2 obtained by Mahadevan et al. [20] (Fig. 8) from first principle calculations. The value of J_2 for four layers is large because it has smaller interlayer separation between Mn-doped GaAs layers than the other cases.

Table 1: Total energies and the interatomic exchange parameters for different number of layers grown along z-direction for 50% Mn coverage in a single layer of GaAs.

No. of layers (atoms)	Energy of FM configuration (eV)	Energy of AFM configuration (eV)	J_2 (eV)
4 (16)	-71.800	-71.602	0.0124
8 (32)	-138.275	-138.266	0.00056
12 (48)	-204.749	-204.720	0.00181
16 (64)	-271.220	-271.164	0.00350

Mn *d* projected partial density of states (DOS) have been shown in Fig.6 as a function of number of layers. The solid lines represent the up spin DOS and dotted lines represent the down spin DOS. The Fermi energy has been set at zero on the energy axis. Examining the density of states one can see that the Mn *d* up-spin density of states lie deep inside the valence band. At Fermi level, the Mn introduces states which are 100% spin polarized and it introduces hole states which lie in the partially filled impurity band.

To see the effect of spin polarization on As ions, the magnetic moment on As ions has been plotted as a function of distance from the Mn (Fig.7) and as expected, it decreases as one goes away from the Mn. From this plot one can say that the magnetic moment on As extends up to fourth layer in the heterostructures.

2. Considering the 2nd case of Mn arrangements on a surface of GaAs heterostructure as shown in Fig.1(c), (d) and (e), the ground state energies have been calculated using *ab-initio* calculations. The interatomic exchange parameters *J*1 and *J*3, which have been shown in Fig.1, have been evaluated using equations (5), (6) and (7). Here also we can see that FM configurations are energetically more stable than the AFM ones. The sign of J_1 is coming out to be positive indicating ferromagnetic exchange whereas, J_3 is coming out to be negative indicating anti-ferromagnetic exchange. If we compare the sign of J_2 and J_3 with the Fig.8, we can see the sign of J_2 is matching with the previous result, whereas the sign of J_3 is opposite.

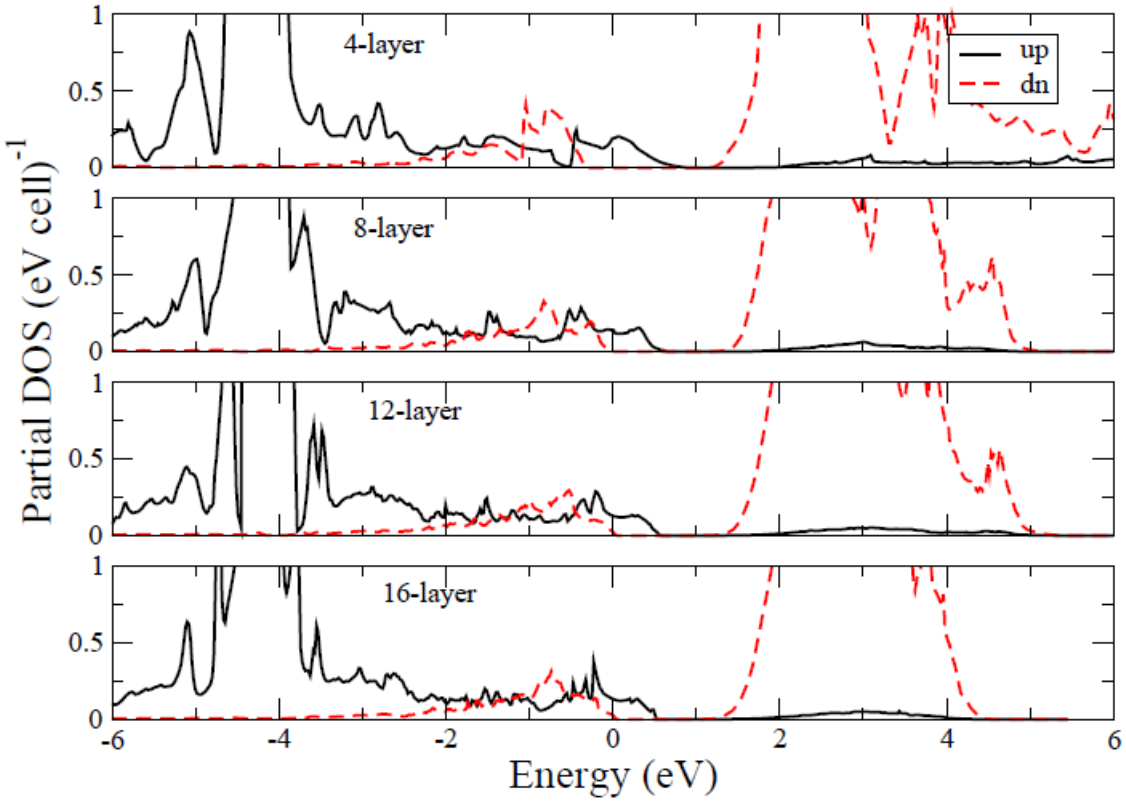

Figure 6: Mn *d* projected partial density of states (DOS) have been plotted as a function of layer thickness.The up spin DOS have been indicated by solid lines and the down spin DOS have been indicated by dashed lines.The Fermi energy has been set at zero on the energy axis.

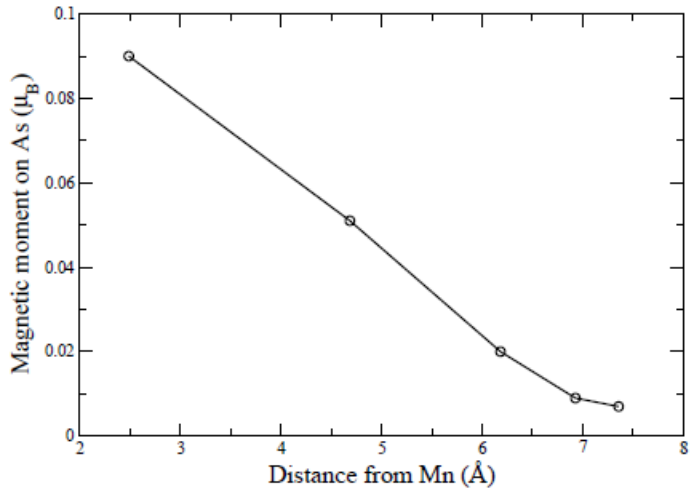

Figure 7: Magnetic moment on As atoms have been plotted as a function of distance from the Mn atom.Magnetic moment on As atom decreases as a function of distance away from the Mn atom.

3. Consider the 3rd type of Mn arrangements, named as chalcopyrite structure (Fig.1 (f), (g) and (h)), on the surface of (Ga,Mn)As heterostructures. The total energies for various configurations for different layers have been calculated from ab-initio calculations and hence the exchange parameters have been evaluated by using equations (8), (9) and (10) and are given in the Table.3. Ferro-magnetic ground states have come out to be more stable than the antiferromagnetic ones.

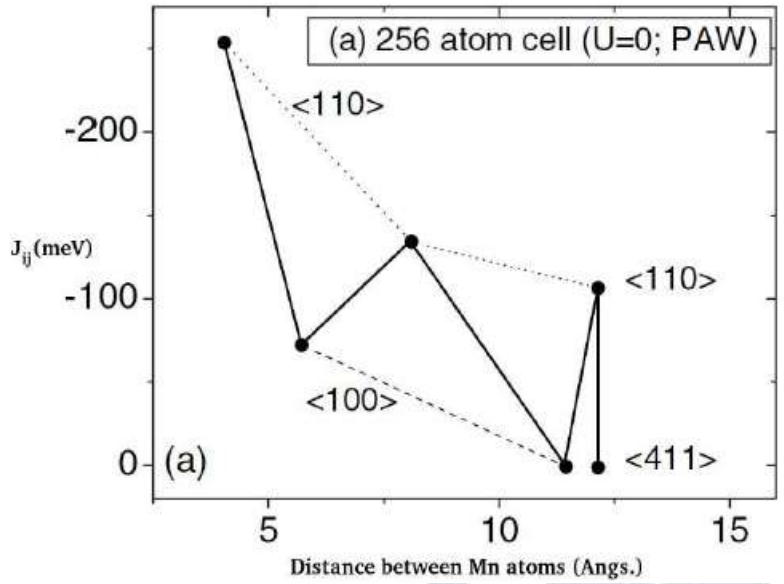

Figure 8: The distance/ orientation dependence of *Ji j* for Mn pairs in a 264 atom GaAs cell using PAWpotentials (Taken from 'Phys. Rev. Lett. **93**, 17(2004)') [20].

Table 2 Total energies and the interatomic exchange parameters for different number of layers grown along z-direction for 50% Mn coverage in a single layer of (Ga,Mn)As.

No. of layers (atoms)	Energy of FM (eV)	Energy of AFM1 (eV)	Energy of AFM2 (eV)	J_1(eV)	J_3(eV)
4 (32)	-143.776	-143.582	-143.242	0.06675	-0.00456
8 (64)	-276.780	-276.596	-276.374	0.05075	-0.00119
12 (96)	-409.740	-409.562	-409.334	0.05075	-0.00156

Both the inter-atomic exchange parameters J_1 and J_2 have been seen to be positive indicating ferromagnetic exchange. Comparing the values of J_1 for this case with the J_1 obtained in Table.2, one can say that the values of J_1 are larger in Table 2. This determines the error bars of our calculations. Looking at the value of J_2 for different number of layers in this case, this is similar as that of in Table 1; we can say that J_2 is one order smaller than the value of J_1.

4. For the fourth type of Mn arrangements as shown in the Fig.2 (a), (b) and (c), the total energies for different magnetic configurations are calculated from the *ab-initio* calculations and hence the exchange parameters are evaluated using equations (11), (12) and (13) and are given in Table 4.

Table 3: Total energies and the interatomic exchange parameters for different number of layers in chalcopyrite structural arrangement for 50% Mn coverage in a single layer of (Ga,Mn)As.

No. of layers (atoms)	Energy of FM (eV)	Energy of AFM1 (eV)	Energy of AFM2 (eV)	*J*1 (eV)	*J*3 (eV)
4 (32)	-143.772	-143.378	-143.256	0.0645	0.0170
8 (64)	-276.780	-276.531	-276.172	0.0760	0.00688
12 (96)	-409.718	-409.454	-409.136	0.0730	0.00365

Table 4: Total energies and the interatomic exchange parameters for different number of layers grown along [110] direction for 50% Mn coverage in a single layer of (Ga,Mn)As.

No. of layers (atoms)	Energy of FM (eV)	Energy of AFM1 (eV)	Energy of AFM2 (eV)	*J*1 (eV)	*J*3 (eV)
4 (32)	-143.797	-143.443	-143.278	0.0648	0.0236
8 (64)	-276.785	-276.538	-276.300	0.0606	0.0011
12 (96)	-409.743	-409.494	-409.274	0.0586	0.0036

The ferromagnetic state is found to be energetically more favorable than the antiferromagnetic ones.

5. We also have considered the case of 25% Mn doping in a single monolayer of GaAs. First we have taken the arrangements as shown in Fig.3 (a) and (b). The ground state energies of FM and AFM arrangements have been calculated using *ab-initio* calculations. The interatomic exchange parameters have been evaluated by using equations (14) and (15) we have calculated the exchange parameters using the calculated total energies from the first-principle calculations as given in the Table 5. From this table, we can say that the value of J_1 has been enhanced compared to 50% doping case.

Table 5 Total energies and the interatomic exchange parameters for different number of layers for 25% Mn coverage in a single layer of (Ga,Mn)As as shown in Fig.3(a), (b).

No. of layers (atoms)	Energy of FM configuration (eV)	Energy of AFM configuration (eV)	J_1 (eV)
2 (32)	-138.335	-138.127	0.104
4 (64)	-271.315	-271.148	0.084

(6) The next type of Mn arrangements, what we have considered, within 25% Mn coverage in a monolayer of GaAs have been shown in Fig.3(c) and (d). The ground state energies have been calculated by ab-initio calculations and hence the interatomic exchange parameters have been evaluated by using equations (16) and (17). Here the value of *J*2 decreases as we have doubled the layer thickness.

Table 6 Total energies and the interatomic exchange parameters for different number of layers for 25% Mn coverage in a single layer of (Ga,Mn)As as shown in Fig.3(c), (d).

No. of layers (atoms)	Energy of FM configuration (eV)	Energy of AFM configuration (eV)	J_1(eV)
2 (32)	-138.246	-138.095	0.076
4 (64)	-271.315	-271.148	0.011

7. The other types of Mn arrangements, we have considered, have been shown in Fig.4. The ground state energies for FM and AFM configurations for different number of layers have been calculated by *ab-initio* calculations. The interatomic exchange parameters (J_3) have been calculated from the ground state total energies using equations (18) and (19). The value of J_3 is coming out to be negative and its magnitude is decreasing as a function of layer thickness. Negative sign of J_3indicates anti ferromagnetic coupling between the magnetic ions within 25% doping concentration.

Table 7: Total energies and the interatomic exchange parameters for different number of layers for 25% Mn coverage in a single layer of GaAs as shown in Fig.4 (a), (b).

No. of layers (atoms)	Energy of FM configuration (eV)	Energy of AFM configuration (eV)	J_3(eV)
2 (32)	-138.260	-138.131	-0.032
4 (64)	-271.249	-271.138 -0.028	-0.028

8. Then we move on to 12.5% doping of Mn in a monolayer of GaAs heterostructure. The ground state energies of different types of magnetic configurations, what we have considered here as shown in Fig.5 (a) and (b), have been calculated by using ab-initio calculations. The exchange parameter J_1 has been estimated for different number of layers using equations (20) and (21) and tabulated in Table 8. Here also the FM configuration has come out to be energetically more favorable than the AFM one as previous cases. J_1 is found to decrease with the number of layers. Comparing the value of J_1 with that of Table 5, we can say that the values of J_1 is almost same for both 25% and 12.5% δ□-doping cases, that is, J_1 is almost saturating down to 12.5% □□-doping concentration.

Table 8: Total energies and the interatomic exchange parameters for different number of layers for 12.5% Mn coverage in a single layer of (Ga,Mn)As as shown in Fig.5(a), (b).

No. of layers (atoms)	Energy of FM configuration (eV)	Energy of AFM configuration (eV)	J_1 (eV)
2 (64)	-271.256	-271.052	0.102
4 (128)	-537.194	-537.039	0.078

9. Within 12.5% doping, we also have considered another type of Mn arrangement in a monolayer as shown in Fig.5 (c) and (d) for FM and AFM configurations respectively. The ground state energies for each of the configurations have been calculated from *ab-initio* calculations and hence the exchange parameters J_2 for different number of layers has been evaluated by using equations (22) and (23) and have been shown in Table 9. The value of J_2 has been seen to decrease as the number of layers increases.

Table 9: Total energies and the interatomic exchange parameters for different number of layers for 12.5% Mn coverage in a single layer of (Ga,Mn)As as shown in Fig.5(c), (d).

No. of layers (atoms)	Energy of FM configuration (eV)	Energy of AFM configuration (eV)	J_2 (eV)
2 (64)	-271.174	-271.051	0.062
4 (128)	-537.100	-537.084	0.008

IV. CONCLUSIONS

In this context, we have calculated the inter-atomic exchange parameters for Mn δ-doped GaAs heterostructures as a function of layer thickness. The inter-atomic exchange parameters J_1 and J_3 have been come out to be larger in dilute doping cases compared to the larger Mn coverage cases. For 50% δ- doping case the exchange parameter $J1$ has been found to be 60 ± 10 meV. This increases to 90 ± 10 meV at 12.5% doping. The induced magnetic moment on As has been found to die down as one goes beyond four monolayers from the Mn δ-doping layer.

V. ACKNOWLEDGEMENT

The authors thank Priya Mahadevan for her proper guiding to do this work.

VI. REFERENCES

[1] H. Ohno, Science **281**, 951(1998).

[2] G.A. Prinz, Science **282**, 1660(1998).

[3] R. Fiederling, M. Keim, G. Reuscher, W. Ossau, G. Schmidt, A.Waag, L.W. Molenkamp, Nature **402**, 787(1999).

[4] Y. Ohno, D.K. Young, B. Beschoten, F. Matsukura, H. Ohno, D.D. Awschalom, Nature **402**, 790(1999).

[5] F. Matsukura, H. Ohno, A. Shen, Y. Sugawara, Phys. Rev. B **57**, R2037(1998).

[6] B. Lee, T. Jungwirth, A. H. MacDonald, Phys. Rev. B, **61**, 23(2000).

[7] A. M. Nazmul, T. Amemiya, Y. Shuto, S. Sugahara, and M. Tanaka, Phys. Rev. Lett. **95**, 017201(2005).

[8] X. Chen, M. Na, M. Cheon, S. Wang, H. Luo, B. D. McCombe, X. Liu, Y. Sasaki, T. Wojtowicz, J. K. Furdyna, S. J. Potashnik and P. Schiffer, Appl. Phys. Lett. **81**, 3(2002).

[9] S. J. Potashnik, K. C. Ku, S. H. Chun, J. J. Berry, N. Samarth, and P. Schiffer, Appl. Phys. Lett. **79**, 1495(2001).

[10] K. M. Yu, W. Walukiewicz, T. Wojtowicz, I. Kuryliszyn, X. Liu, Y. Sasaki, and J. K. Furdyna, Phys. Rev. B **65**, 201303R(2002).

[11] J. Blinowski and P. Kacman, Phys. Rev. B **67**, 121204R(2003).

[12] R. K. Kawakami, E. Johnston-Halperin, L. F. Chen, M. Hanson, N. Guebels, J. S. Speck, A. C. Gossard, and D. D. Awschalom, Appl. Phys. Lett. **77**, 2379(2000).

[13] X. H. Zhou, Xiaoshuang Chen, Y. Huang, H. Duan, L. Z. Sun, and W. Lu, J. Appl. Phys. **99**, 113903(2006).

[14] N. Akiba, F. Matsukura, A. Shen, Y. Ohno, H. Ohno, A. Oiwa, S. Katsumoto, and Y. Iye, Appl. Phys. Lett. **73**, 2122 (1998).

[15] International Crystal Structure Database.